Neutron-induced fission cross sections of ^{233}U and ^{243}Am in the energy range 0.5 Mev$\leq$ E$_n$ $\leq$ 20 MeV @ n_TOF

F. Belloni[1,], P.M. Milazzo[1], M. Calviani[2], N. Colonna[3], P. Mastinu[4], U. Abbondanno[1], G. Aerts[5], H. Álvarez[6], F. Álvarez-Velarde[7], S. Andriamonje[5], J. Andrzejewski[8], P. Assimakopoulos[†9], L. Audouin[10], G. Badurek[11], P. Baumann[12], F. Bečvář[13], E. Berthoumieux[5], F. Calviño[14], D. Cano-Ott[7], R. Capote[15,16], C. Carrapiço[17], P. Cennini[2], V. Chepel[18], E. Chiaveri[2], G. Cortes[19], A. Couture[20], J. Cox[20], M. Dahlfors[2], S. David[10], I. Dillmann[21], C. Domingo-Pardo[21,22], W. Dridi[5], I. Duran[6], C. Eleftheriadis[26], M. Embid-Segura[7], L. Ferrant[†10], A. Ferrari[2], R. Ferreira-Marques[18], K. Fujii[1], W. Furman[24], I. Goncalves[18], E. González-Romero[7], F. Gramegna[4], C. Guerrero[7], F. Gunsing[5], B. Haas[25], R. Haight[26], M. Heil[21], A. Herrera-Martinez[2], M. Igashira[27], E. Jericha[11], F. Käppeler[21], Y. Kadi[2], D. Karadimos[9], D. Karamanis[9], M. Kerveno[12], P. Koehler[28], E. Kossionides[29], M. Krtička[13], C. Lampoudis[5,23], H. Leeb[11], A. Lindote[18], I. Lopes[18], M. Lozano[16], S. Lukic[12], J. Marganiec[8], S. Marrone[3], T. Martínez[7], C. Massimi[30], A. Mengoni[2,15], C. Moreau[1], M. Mosconi[21], F. Neves[18], H. Oberhummer[11], S. O'Brien[20], J. Pancin[5], C. Papachristodoulou[9], C. Papadopoulos[31], C. Paradela[6], N. Patronis[9], A. Pavlik[32], P. Pavlopoulos[33], L. Perrot[5], M.T. Pigni[11], R. Plag[21], A. Plompen[34], A. Plukis[5], A. Poch[19], J. Praena[16], C. Pretel[19], J. Quesada[16], T. Rauscher[35], R. Reifarth[26], C. Rubbia[36], G. Rudolf[12], P. Rullhusen[34], J. Salgado[17], C. Santos[17], L. Sarchiapone[2], I. Savvidis[23], C. Stephan[10], G. Tagliente[3], J.L. Tain[22], L. Tassan-Got[10], L. Tavora[17], R. Terlizzi[3], G. Vannini[30], P. Vazl[17], A. Ventura[37], D. Villamarin[7], M.C. Vincente[7], V. Vlachoudis[2], R. Vlastou[31], F. Voss[21], S. Walter[21], M. Wiescher[20], K. Wisshak[21]*

The n_TOF Collaboration(www.cern.ch/ntof)

[1]Istituto Nazionale di Fisica Nucleare, Trieste, Italy - [2]CERN, Geneva, Switzerland - [3]Istituto Nazionale di Fisica Nucleare, Bari, Italy - [4]Istituto Nazionale di Fisica Nucleare, Laboratori Nazionali di Legnaro, Italy - [5]CEA/Saclay - IRFU, Gif-sur-Yvette, France - [6]Universidade de Santiago de Compostela, Spain - [7]Centro de Investigaciones Energeticas Medioambientales y Tecnologicas, Madrid, Spain - [8]University of Lodz, Lodz, Poland - [9]University of Ioannina, Greece - [10]Centre National de la Recherche Scientifique/IN2P3 - IPN, Orsay, France - [11]Atominstitut der Österreichischen Universitäten, Technische Universität Wien, Austria - [12]Centre National de la Recherche Scientifique/IN2P3 - IReS, Strasbourg, France - [13]Charles University, Prague, Czech Republic - [14]Universidad Politecnica de Madrid, Spain - [15]International Atomic Energy Agency (IAEA), Nuclear Data Section, Vienna, Austria, [16]Universidad de Sevilla, Spain - [17]Instituto Tecnológico e Nuclear(ITN), Lisbon, Portugal - [18]LIP - Coimbra & Departamento de Fisica da Universidade de Coimbra, Portugal - [19]Universitat Politecnica de Catalunya, Barcelona, Spain - [20]University of Notre Dame, Notre Dame, USA - [21]Forschungszentrum Karlsruhe GmbH (FZK), Institut für Kernphysik, Germany - [22]Instituto de Física Corpuscular, CSIC-Universidad de Valencia, Spain - [23]Aristotle University of Thessaloniki, Greece - [24]Joint Institute for Nuclear Research, Frank Laboratory of Neutron Physics, Dubna, Russia - [25]Centre National de la Recherche Scientifique/IN2P3 - CENBG, Bordeaux,France - [26]Los Alamos National Laboratory, New Mexico, USA - [27]Tokyo Institute of Technology, Tokyo, Japan - [28] Oak Ridge National Laboratory, Physics Division, Oak Ridge, USA - [29]NCSR, Athens, Greece - [30]Dipartimento di Fisica, Università di Bologna, and Sezione INFN di Bologna, Italy - [31] National Technical University of Athens, Greece - [32]Institut für Isotopenforschung und Kernphysik, Universität Wien, Austria - [33]Pôle Universitaire Léonard de Vinci, Paris La Défense, France - [34]CEC-JRC-IRMM, Geel, Belgium - [35]Department of Physics - University of Basel, Switzerland - [36]Università degli Studi Pavia, Pavia, Italy - [37]ENEA, Bologna, Italy

Abstract

Neutron-induced fission cross-sections of actinides have been recently measured at the neutron time of flight facility n_TOF at CERN in the frame of a research project involving isotopes relevant for nuclear astrophysics and nuclear technologies. Fission fragments are detected by a gas counter with good discrimination between nuclear fission products and background events. Neutron-induced fission cross-sections of ^{233}U and ^{243}Am were determined relative to ^{235}U. The present paper reports the results obtained at neutron energies between 0.5 and 20 MeV.

1 Introduction

Precise and consistent neutron-induced fission cross-sections of actinides are required for the design of systems based on the Th/U fuel cycle [1], for ADS [2–4], and Gen-IV nuclear reactors [5]. More accurate fission cross-sections are required - among other physical parameters - to reach higher fuel burn-up, thus increasing the efficiency of the fuel cycle, and to improve the safety of future systems, which aim at a higher actinide fraction in the fuel mix.

An extensive measurement campaign for reducing the $\sigma_{(n,f)}$ uncertainties for major and minor actinide isotopes has been carried out at the n_TOF neutron time of flight facility. In this contribution we report on the ^{233}U and ^{243}Am (n,f) cross-sections from 500 keV up to 20 MeV.

*Presenting author,e-mail: francesca.belloni@ts.infn.it

For ^{243}Am $\sigma_{(n,f)}$, discrepancies between data from different measurements reach 15% in the fast energy region of the incident neutron spectrum [19–22]. A working party on International Evaluation Co-operation has been established by the OECD/NEA nuclear science committee [6]. A study to evaluate the impact of neutron cross section uncertainties on some integral parameters (like criticality) was performed for the core and fuel cycle of generation IV reactors. The most stringent requirements for the ^{243}Am (n,f) cross section were found for Advanced Minor Actinides Burners (ADMAB), where the reduction of the uncertainty by a factor 5 is requested between 0.490 and 6.07 MeV (Table 1).

Table 1: ADMAB Target Accuracy Results

Isotope	Cross Section	Energy Range	Uncertainty (%)	
		(MeV)	Initial	Required
^{243}Am	σ_{fiss}	6.07-2.23	11.0	2.3
		2.23-1.35	6.0	1.9
		1.35-0.498	11.0	2.3

[a] For details see Table 23 in Ref. [6].

The ^{233}U (n,f) cross section is crucial for the study of the Th/U fuel cycle, which is of interest due to the abundance of the ^{232}Th seed and for the reduced production of long-lived actinides. The Th-U fuel cycle ends up with a lower production of MAs with respect to the U-Pu fuel cycle and the produced U represents a useful fuel as well. This cycle is characterized by its intrinsic proliferation resistance, because the ^{232}U produced via ^{233}U(n,2n) reactions decays rapidly to strong γ emitters and makes, therefore, the handling of the fuel containing ^{233}U more difficult.

2 The n_TOF Facility

The n_TOF (neutron Time Of Flight) facility [7] is a high fluence spallation neutron source. Neutrons are produced in a thick lead target ($60 \times 80 \times 80$ cm^3) by short proton pulses of 20 GeV/c momentum and 6 ns r.m.s., giving rise to a high neutron flux (about 300 neutrons are produced per incident proton) in a wide energy range from 1eV to 250 MeV. From the spallation target, an evacuated neutron beam line leads to the Experimental Area (EAR1) at a distance of 185 m. Along this beam line massive concrete and iron shieldings as well as a sweeping magnet are used in order to reduce the background due to the intense γ-flash and to relativistic charged particles from the spallation source.

The experimental area contains several detectors for capture and fission studies, which are normally performed with different beam diameters and different beam monitors. For a list of the available detectors see Ref. [8]. Behind the experimental area, the beam line continues for another 12 m before it ends in a beam-dump to avoid background from backscattered neutrons.

3 The Fast Ionization Chamber

Measurements of neutron-induced fission cross-sections have been carried out using Fast Ionization Chambers (FIC) [10, 11] built by a collaboration between the Joint Institute of Nuclear Research (JINR, Dubna, Russian Federation), the Institute of Physics and Power Engineering (IPPE, Obninsk, Russian Federation), INFN, and CERN. Two identical chambers were designed for samples with high and low α-activities, respectively, and a third was intended for ^{235}U and ^{238}U samples to be used as a flux monitor.

A simplified layout of the FIC is shown in Fig. 1. The basic cell is composed of three aluminum electrodes 12 cm in diameter. The central electrode is 100 μm in thickness and is plated on both sides with the fissile isotope under study. This central electrode is connected to the bias voltage for defining the electric field of 600 V/cm in the 5 mm wide gas-filled gaps. The two outer electrodes 15 μm in thickness are kept at ground potential. The sample layers are 8 cm in diameter. The whole detector is 50 cm long and houses up to 17 basic cells perpendicular to the neutron beam. The samples investigated in this work are listed in Table 2.

Signals produced by fission fragments in the sensitive gas volume are proportional to the specific energy loss of the fragments, which is a function of their atomic number. Given the 2π geometry of the chamber, the detection efficiency for fission events is close to 100% for each cell. In order to fulfil the safety regulations at CERN, the FIC is operated in the ionization regime, without gas flow. The chamber is therefore operated as a sealed detector at a pressure of 720 mbar. Because of the high α-activity of the samples, a gas mixture of 90% Ar + 10% CF_4 was used to ensure fast charge collection (t $\leq$ 50 μs). This was essential for minimizing α pile-up and dead time effects.

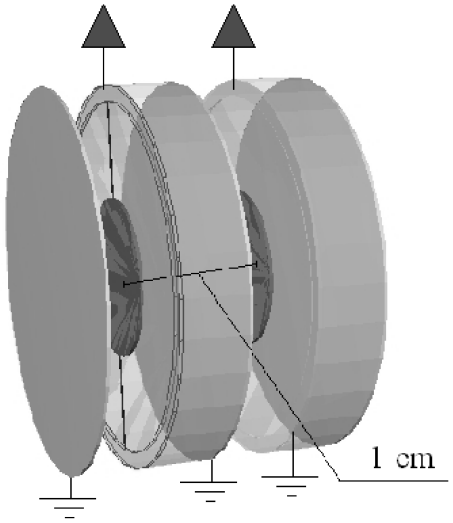

Fig. 1: Schematic layout of four FIC cells

Table 2: Total sample mass

Isotope	Mass (mg)
^{233}U	30.84 ± 0.37
^{235}U	31.80 ± 0.43
^{243}Am	4.78 ± 0.06

4 Data Analysis

4.1 Cross sections

Cross Sections are extracted relative to ^{235} U, which is a standard between 0.15 MeV and 200 MeV. At high energy, signals are strongly affected by the so-called γ-flash produced by prompt γ-rays and relativistic particles originating from spallation reactions in the Pb target. In the FIC, the high intensity of the γ-flash causes strong oscillations in the output signal.

The strong fluctuations in the time evolution of the signal amplitude are shown in the left Panel of Fig. 2. The problem can be solved, up to a given energy, by observing that two adjacent electrodes are affected by the γ-flash in the same way. Therefore, a software compensation technique can be applied in order to extract the signals of fission fragments. The technique consists in subtracting the output of two adjacent electrodes [9]. The results of this procedure is illustrated in the right Panel of Fig. 2. The signals are then subjected to a pulse shape analysis and to an amplitude threshold in order to discriminate between fission fragments and α particles (Fig. 3). Residual electronic noise is reduced by considering the charge-to-amplitude ratio of the signals. The TOF information was converted to an energy scale by defining the so-called "time zero" (t_0) by means of the γ-flash. Although the samples are separated by 10 mm, a common flight-path was used in the analysis. The corresponding uncertainty of about 0.3% in neutron energy introduced in this way is negligible in view of the smooth cross section trend in the MeV region.

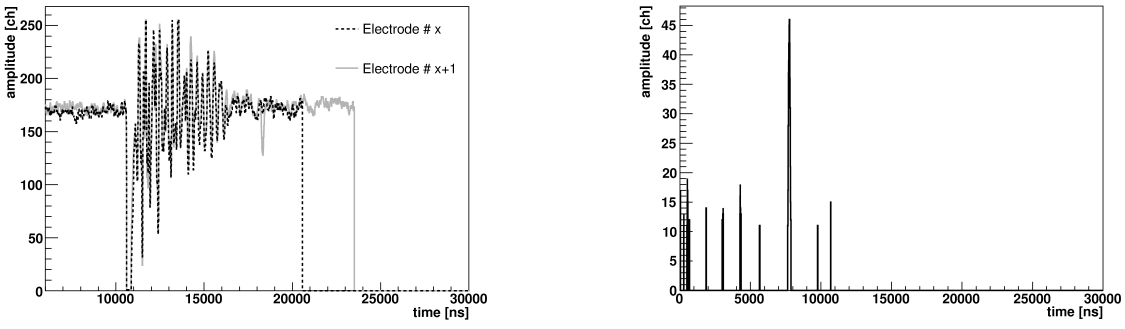

Fig. 2: (Left) Recorded raw signals from neighboring electrodes. (Right) Signals after subtraction of cross-talk and γ-flash.

The neutron-induced fission cross-sections are extracted according to the following expression:

$$\sigma_{xxx(n,f)} = \sigma_{235(n,f)} \cdot \frac{N_{xxx}}{N_{235}} \cdot \frac{m_{235}}{m_{xxx}} \cdot \frac{A_{xxx}}{A_{235}} \, . \tag{1}$$

where

– $\sigma_{235(n,f)}$ is the tabulated ENDF/B-VII.0 cross section,
– xxx stands for the investigated isotope, i.e. ^{233}U or ^{243}Am,
– N_{xxx} denotes the number of fission events detected for isotope xxx
– m_{xxx} is the mass (in grams) of isotope xxx,
– A_{xxx} is the atomic number of isotope xxx

Since the investigated isotopes and the ^{235}U reference samples are mounted in the same detector, they are exposed to the same neutron flux.

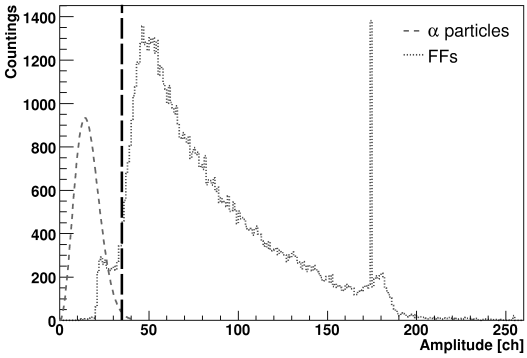

Fig. 3: Experimental pulse height spectrum for ^{235}U. The vertical line indicates the threshold chosen to discriminate between α particles and fission fragments. The peak at channel 185 is due to saturation effects.

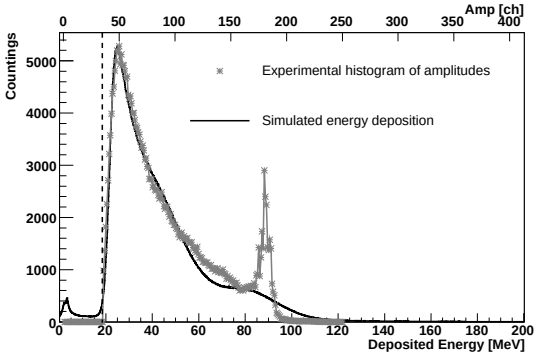

Fig. 4: Simulation of the energy deposited by fission fragments in the FIC folded with an energy resolution of 15% and normalized to the measured pulse height spectrum. The threshold at channel 35 corresponds to an energy of about 18 MeV.

4.2 Corrections

The number of detected fission events obtained by Eq. 1 had to be corrected for dead-time and detection efficiency.

The dead time of a counting system can be treated by assuming a paralysable or a non-paralysable response. In the non-paralysable mode a fixed dead time is assumed for each recorded event. Signal falling in this time window are lost, so that a correction has to be applied in the extracted cross-section. A non-paralysable model has been used in the present analysis, with the dead-time (of 300 ns) related to the signal reconstruction routine. For most of the measured isotopes, the dead-time correction goes from a few percent at low energy, to 20% at higher energy. However, since the count-rate in the various isotopes is similar, the corrections mostly cancel out in the ratio, with a residual effect of the order of a few percent, with a corresponding uncertainty less than 1%.

Another correction that needs to be applied in extracting the cross-section is related to the detection efficiency. The number of particles leaving the sample as well as the spectrum of energy loss in the gas volume, is determined by the sample thickness, so that differences in the detection efficiency may exist for the different measured isotopes. The effect of fragment absorption in the sample thickness was estimated by simulating the energy loss of fission fragments in the sample deposit and in the gas with the FLUKA code [13]. The simulated distributions of the energy deposited by the fission fragment in the gas volume of the chamber were folded with an energy resolution of 15% to match the measured pulse height spectrum as shown in Fig. 4. In this way, the detection efficiency can be calculated for each isotope, taking into account the threshold applied on the measured amplidute distribution. For all isotopes here shown, the simulated efficiency is very high, ranging between 95% for ^{235}U and 98% for ^{243}Am. Therefore, when extracting the cross-section for the various isotopes relative to ^{235}U, a correction of only a few percent has to be applied. Consequently, the uncertainty related to the detection efficiency is below 1%. Considering all effects and corrections introduced in extracting the cross-sections, the overall systematic uncertainty on the extracted cross-section for the two isotopes here investigated is slightly higher than 4%, mostly determined by the uncertainty on the mass of the various deposits (including the ^{235}U sample used as reference).

5 Results

Although the energy range covered by the present measurements extends to 200 MeV, fission cross sections are reported here only up to 20 MeV. Results obtained at higher energies are at present largely affected by the γ flash and, therefore, still preliminary.

5.1 ^{233}U

The results of the present measurements are shown in Fig. 5 compared to experimental data by Tovesson *et al.* [14], Shcherbakov *et al.* [15], Lisowski *et al.* [16], Fursov *et al.* [17], and Grosjean *et al.* [18]. In general, fairly good agreement is found with the data of Lisowski *et al.* [16] and Tovesson *et al.* [14], whereas the values of Fursov *et al.* are slightly lower. Below 10 MeV, the n_TOF results are also in good agreement with the ENDF/B-VII.0 evaluation (see Fig. 6), although below 1 MeV the evaluated cross-sections are systematically lower than the n_TOF results, by approximatelly 5%.

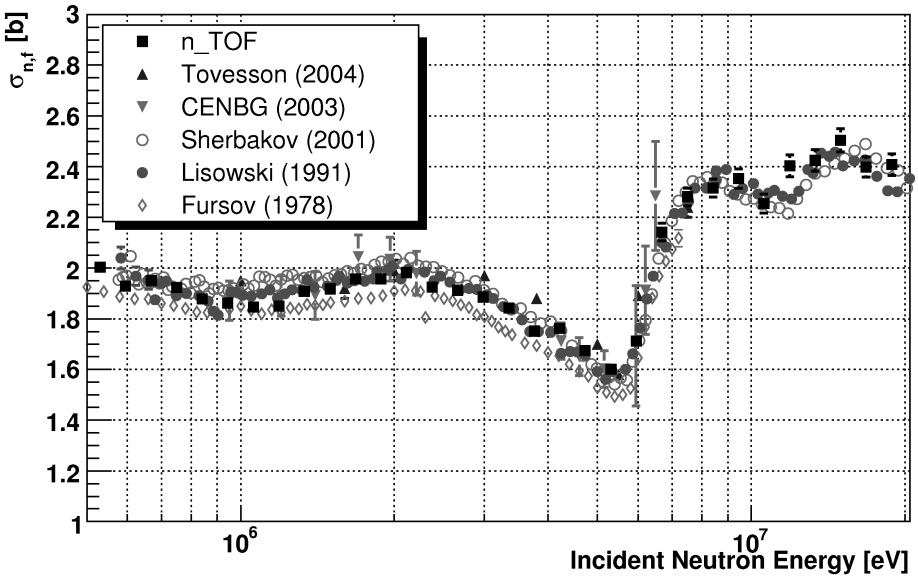

Fig. 5: Comparison among present results for ^{233}U and previous data.

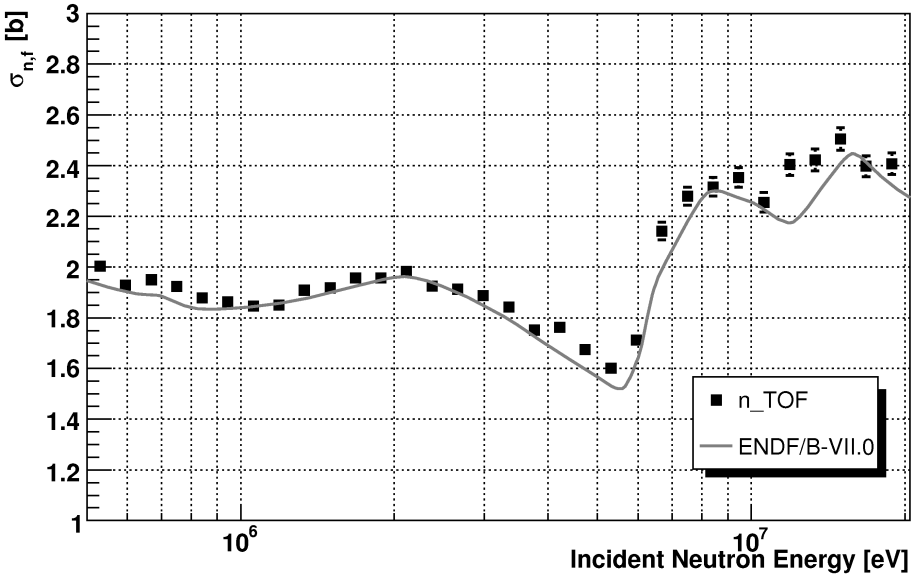

Fig. 6: Comparison between present results and the ENDF/B-VII.0 evaluation.

The comparison with previous experiments and evaluations is summarized in Table 3, which lists the ratio of the n_TOF results over previous data, integrated in the indicated energy region.

Table 3: Difference between present results for ^{233}U and previous data.

Author/library	Range of integration (MeV)	Difference (%)
Fursov *et al.* [17]	0.3 - 7.4	+2.4
Shcherbakov *et al.* [15]	0.577 - 20.0	+0.9
Lisowski *et al.* [16]	0.583 - 20.0	+1.2
Tovesson *et al.* [14]	1.0 - 7.5	-2.1
CENBG[a]	0.950 - 6.49	-0.7
ENDF/B-VI.8	0.3 - 20.0	+5.6
JEFF 3.1	0.3 - 20.0	+3.5
ENDF/B-VII.0	0.3 - 30.0	+4.8
JENDL	0.3 - 20.0	+3.5

[a] Centre d'Etudes Nucleaires de Bordeaux Gradignan

5.2 ^{243}Am

A comparison between the present measurement and the results of Aiche *et al.* [19], Laptev *et al.* [20], Seeger *et al.* [21], and Fursov *et al.* [22] is shown in Fig 7. The present results from n_TOF confirm that the data of Laptev *et al.* are systematically too high. A good agreement is observed between n_TOF data and other previous measurements. A reasonable agreement is also observed between the present results and the ENDF/B-VII.0 compilation below 10 MeV (Fig 8). A summary of the comparison between n_TOF cross-sections and previous data and evaluation can be found in Table 4.

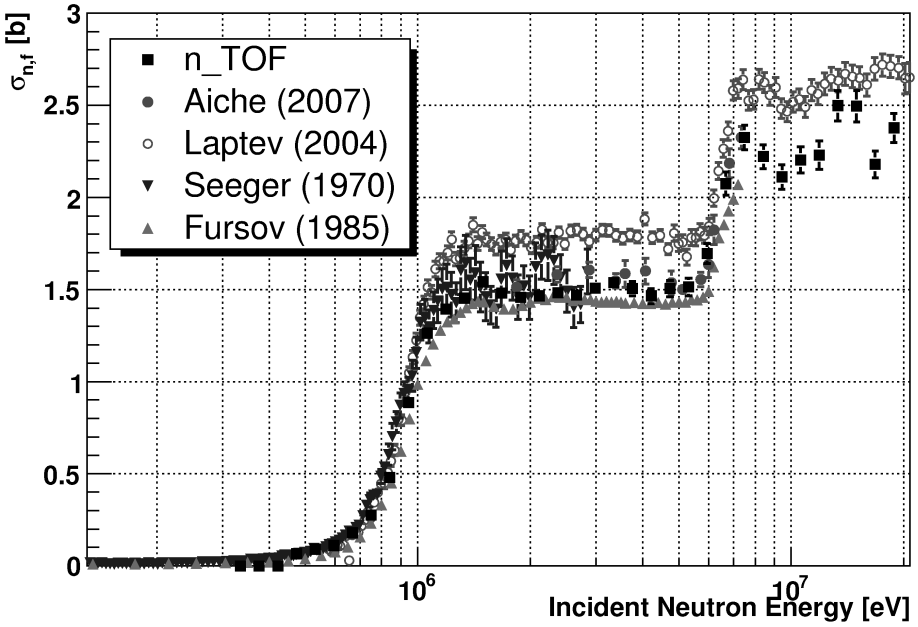

Fig. 7: Comparison between present results for ^{243}Am and previous data.

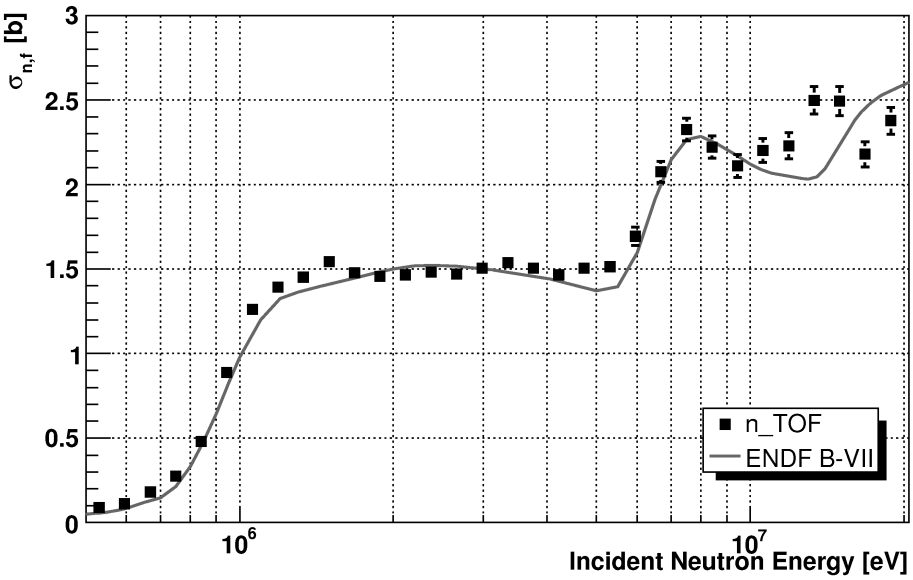

Fig. 8: Comparison between present results for ^{243}Am and the ENDF/B-VII.0 evaluation.

Table 4: Difference between present results for ^{243}Am and previous data.

Author/library	Range of integration (MeV)	Difference (%)
Seeger *et al.* [21]	0.3 - 2.97	-5.9
Aiche *et al.* [19]	1.34 - 7.35	-2.4
Fursov *et al.* [22]	0.3- 7.4	+6.3
Laptev *et al.* [20]	0.577 - 20.0	-14.5
ENDF/B-VII.0	0.3 - 30.0	-0.5
JEFF 3.1	0.3 - 20.0	+6.1
BROND2.2	0.3 - 30.0	+4.9
JENDL-AC-2008	0.3 - 20.0	+7.3

5.3 Conclusions

Taking advantage of the high instantaneous flux and the high energy resolution of the CERN n_TOF facility, neutron-induced fission cross-sections of ^{233}U and ^{243}Am have been measured in the energy range between 0.5 MeV and 20 MeV relative to ^{235}U as a standard, using a Fast Ionization Chamber. To minimize systematic errors, all samples were mounted in the same chamber and measured simultaneously. Corrections for dead-time and detection efficiency have been included in the analysis, in order to extract cross-section with a high accuracy. The overall uncertainty in the present results is 4% in the whole enery region here reported. A comparison with previous data and evaluations for ^{233}U shows differences of the less than 10%. Some revision of the current databases, in particular below 1 MeV, is needed to account for the new results. For ^{243}Am, the n_TOF data confirm the results of Fursov and agree reasonably well with the current evaluation, while confirming that recent data from Laptev were overstimating the cross-section by as much as 15%. The results here presented are important to resolve discrepancies in previous data, thus providing a reliable basis for future evaluations to be used for the design and safe operation of advanced nuclear system.

References

[1] *Th fuel cycle - potential benefits and challenges*, IAEA-TECDOC-1450 (2005).

[2] Bowman *et al.*, Nucl. Instrum. Methods, A **320**, 336 (1992).

[3] F. Carminati, C. Gels, R. Klapisch, P. Revol, Ch. Roche, J. A. Rubio and C. Rubbia, *An energy amplifier for cleaner and inexhaustible nuclear energy production driven by a particle beam accelerator*, CERN/AT/93-47(ET) (1993).

[4] C. Rubbia, J.A. Rubio, S. Buono, F. Carminati, N. Fitier, J. Galvez, C. Gels, Y. Kadi, R. Klapish, P. Mandrillon, J.P. Revol,and Ch. Roche, *Conceptual design of a fast neutron operated high power energy apmlifier*, CERN/AT/95-44(ET) 1995.

[5] US DOE Nuclear Energy Research Advisory Committee, *A technology roadmap for generation IV nuclear energy systems* (2002).

[6] M. Salvatores, *Uncertainty and target accuracy assessment for innovative systems using recent covariance data evaluations*, Nucl. Sc. NEA/WPEC-26 (2008), available at www.nea.fr/html/science/wpec/volume26/volume26.pdf.

[7] All documents describing the facility are available at www.cern.ch/ntof.

[8] F. Gunsing *et al.*, *Neutron resonance spectroscopy at n_TOF at CERN*, in Nuclear Data for Science and Technology, eds. O. Bersillon *et al.* (EDP Sciences, Les Ulis, 2007) 537.

[9] N.Colonna, M. Calviani *et al. Nucl. Inst. and Meth. A*,in preparation

[10] M. Calviani, P. Cennini, D. Karadimos, V. Ketlerov, V. Konovalov, W. Furman, A. Goverdowski, V. Vlauchoudis and L. Zanini, *Nucl. Instrum. Meth.* A **594**, 220 (2008).

[11] *A Detailed Study of the Hyperdeformed States of Uranium in the ^{234}U(n,f) Reaction*. The n_TOF collaboration, CERN/INTC 2002-022, INTC/P145 Add. 1 (2002).

[12] G. Lorusso *et al.*, *Nucl. Instrum. Meth.* A **532**, 622 (2004).

[13] A. Fassò, A. Ferrari, J. Ranft, and P.R. Sala, *FLUKA: a multi-particle transport code* CERN-2005-10 (2005), INFN/TC_05/11, SLAC-R-773, www.fluka.org/fluka.php/.

[14] F. Tovesson *et al.*, *Nucl. Phys.* A **733**, 3 (2004).

[15] O.A. Shcherbakov *et al.*, *J. Nucl. Science and Technology*, Supplement 2, Vol. 1, 230 (2002).

[16] P.W. Lisowski, A. Gavron, W.E. Parker, S.J. Balestrini, A.D. Carlson, O.A. Wasson, N.W. Hill, *Fission cross sections ratios for ^{233,234,236}U relative to ^{235}U from 0.5 to 400 MeV, Nucl. Data for Sci.and Technology*, ed. S. Qaim (Springer, Berlin, 1992) p. 732.

[17] B.I. Fursov, V.M. Kuprijanov, G.N. Smirenkin, *Atomic Energy* **44**, 236 (1978).

[18] Private communication.

[19] M. Aiche *et al.*, *Quasi-absolute neutron-induced fission cross section of ^{243}Am, Nucl. Data for Sci.and Technology*, ed. S. Qaim (Springer, Berlin, 1992) p. 483.

[20] A.V. Laptev *et al.*, *Nucl. Phys.* A **734**, E45 (2004).

[21] P.A. Seeger *Fission cross sections from Pommard*, Los Alamos Sci. Report 4420, p.138 (1970).

[22] B.I. Fursov, E.Ju. Baranov, M.P. Klemyshev, B.F. Samylin, G.N. Smirenkin, Yu.M. Turchin, *Atomic Energy* **59**, 899 (1985).

Bibliography

Glenn F. Knoll, *Radiation detection and measurements* (John Wiley, New York, 1979).